Inorganic Chemistry

Article

pubs.acs.org/IC

Open Access on 07/28/2015

Reaction of an Iron(IV) Nitrido Complex with Cyclohexadienes: Cycloaddition and Hydrogen-Atom Abstraction

Wei-Tsung Lee,[†] Ruth A. Juarez,[‡] Jeremiah J. Scepaniak,[‡,§] Salvador B. Muñoz, III,[†] Diane A. Dickie,[∥] Haobin Wang,*[,‡] and Jeremy M. Smith*[,†]

[†]Department of Chemistry, Indiana University, 800 East Kirkwood Avenue, Bloomington, Indiana 47405, United States

[‡]Department of Chemistry and Biochemistry, New Mexico State University, Las Cruces, New Mexico 88003, United States

[∥]Department of Chemistry and Chemical Biology, The University of New Mexico, Albuquerque, New Mexico 87131, United States

Supporting Information

ABSTRACT: The iron(IV) nitrido complex PhB(MesIm)$_3$Fe≡N reacts with 1,3-cyclohexadiene to yield the iron(II) pyrrolide complex PhB(MesIm)$_3$Fe(η^5-C$_4$H$_4$N) in high yield. The mechanism of product formation is proposed to involve sequential [4 + 1] cycloaddition and retro Diels–Alder reactions. Surprisingly, reaction with 1,4-cyclohexadiene yields the same iron-containing product, albeit in substantially lower yield. The proposed reaction mechanism, supported by electronic structure calculations, involves hydrogen-atom abstraction from 1,4-cyclohexadiene to provide the cyclohexadienyl radical. This radical is an intermediate in substrate isomerization to 1,3-cyclohexadiene, leading to formation of the pyrrolide product.

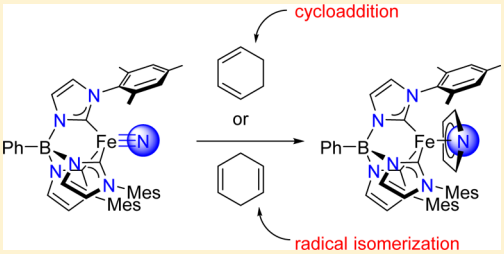

INTRODUCTION

Developing the reactivity of metal ligand multiple bonds toward unsaturated hydrocarbons is important for accessing useful organic molecules in an atom-economical manner. Thus, for example, nonheme iron oxo and imido complexes have been shown to catalytically effect two-electron atom/group transfer to alkenes, generating valuable products such as epoxides[1] and aziridines.[2−4]

In contrast to transition metal oxo and imido complexes, only a small number of nitrido complexes have been observed to react with unsaturated hydrocarbons. In one case, it has been found that addition of pyridine to [(salchda)Ru≡N]$^+$ (salchda = *N*,*N*′-bis(salicylidene)-*o*-cyclohexyldiamine dianion) activates the nitrido ligand toward alkene aziridination,[5] the lone example of a reaction that is analogous to alkene epoxidation by oxo complexes. On the other hand, the reactivity of certain nitrido complexes toward unsaturated hydrocarbons finds no analogue in either oxo or imido chemistry. Pertinent examples include *cis*-[(terpy)Os(N)Cl$_2$]$^+$, which can insert the nitrido ligand into the C=C bond of stilbenes and dienes to form azallenium products,[6] and TpOs(N)Cl$_2$, which undergoes [4 + 1] reactions with 1,3-cyclohexadienes to yield azabicylic complexes.[7]

We previously reported the synthesis and characterization of the iron(IV) nitride complex, PhB(MesIm)$_3$Fe≡N, **1**, Scheme 1.[8] In contrast to many other high-valent iron nitrides,[9] this complex can be isolated, allowing for comprehensive investigations into its reactivity.[10] Initial studies have revealed that the complex is active in two-electron nitrogen-atom transfer reactions with triarylphosphines to provide the corresponding phosphoraniminato complexes PhB(MesIm)$_3$Fe−N=PAr$_3$.[11] Similar two-electron nitrogen-atom transfer reactions to CO and CN^{t}Bu yield the six-coordinate complexes PhB(MesIm)$_3$Fe(NCO)(CO)$_2$ and [PhB(MesIm)$_3$Fe(CN^{t}Bu)$_3$][NCN^{t}Bu], respectively.[12] Complex **1** also reacts in single-electron pathways, including with Gomberg's dimer to provide an iron(III) imido complex and with TEMPO-H to generate ammonia.[8]

In this article, we report reactions of **1** with cyclic dienes, specifically 1,3-cyclohexadiene and 1,4-cyclohexadiene. Surprisingly, with both substrates the same iron pyrrolide product is observed, although only for the reaction with 1,3-cyclohexadiene is formation of this product quantitative. Mechanistic schemes, supported by electronic structure calculations, that account for these observations are presented.

EXPERIMENTAL SECTION

All manipulations were performed under a nitrogen atmosphere by standard Schlenk techniques or in an MBraun Labmaster glovebox. Glassware was dried at 150 °C overnight. Diethyl ether, *n*-pentane, tetrahydrofuran, and toluene were purified by the Glass Contour solvent purification system. Deuterated benzene was first dried with CaH$_2$ and then over Na/benzophenone and then vacuum transferred into a storage container. Before use, an aliquot of each solvent was tested with a drop of sodium benzophenone ketyl in THF solution. All reagents were purchased from commercial vendors and used as received. Deuterated 1,4-cyclohexadiene[13] and PhB(MesIm)Fe≡N, **1**[10] were prepared according to literature procedures. ^{1}H NMR data

Received: May 1, 2014
Published: July 28, 2014

   dx.doi.org/10.1021/ic5010006 | *Inorg. Chem.* 2014, 53, 8425−8430

Scheme 1. Reactions of the Iron(IV) Nitrido Complex, PhB(MesIm)$_3$Fe≡N, 1

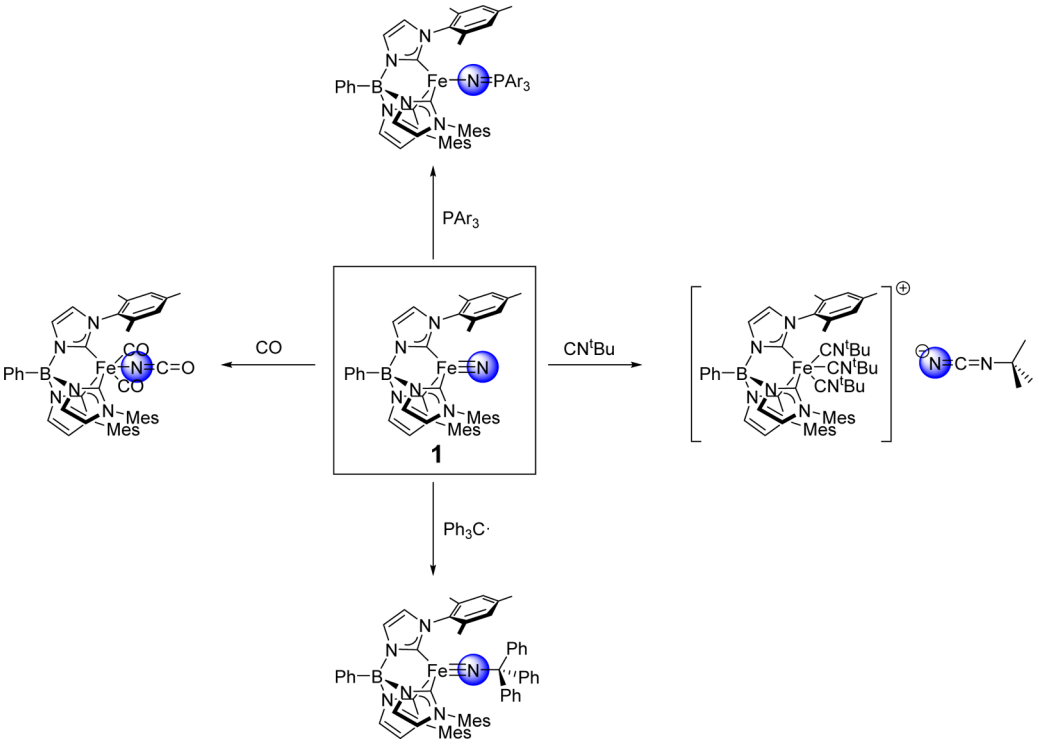

were recorded on a Varian Inova 400 or 500 MHz spectrometer at 25 and 70 °C. Resonances in the ^{1}H NMR spectra are referenced to residual C_6D_5H at δ = 7.16 ppm. UV−vis spectra were recorded on an Agilent Cary 60 UV−vis spectrophotometer equipped with a Unisoku cryostat. GC/MS analysis was performed using an Agilent 6890N gas chromatograph and 5973 inert mass-selective detector equipped with a DB-5MS (Agilent) column (30 m × 0.25 mm). Elemental analysis data were collected by Midwest Microlab, LLC (Indianapolis, IN).

Preparation of PhB(MesIm)$_3$Fe(η^5-C$_4$H$_4$N) 2. Complex **1** (0.1 mmol, 72 mg), 1,3-cyclohexadiene (0.12 mmol, 10 mg), toluene (3 mL), and a magnetic stir bar were added to a bomb flask. The flask was sealed and heated with stirring at 70 °C in an oil bath. Volatiles were removed under reduced pressure, and the residue was extracted with *n*-pentane and filtered through Celite. The filtrate was dried in vacuo to yield an orange solid (65 mg, 85%). Crystals suitable for X-ray diffraction were grown from a concentrated *n*-pentane solution at −30 °C. ^{1}H NMR (500 MHz, C_6D_6, δ): 8.17 (d, J = 5.0, 2H, Ar*H*), 7.43−7.33 (m, 3H, Ar*H*), 7.28 (s, 3H, Ar*H*), 6.77 (s, 6H, Ar*H*), 6.32 (s, 3H, Ar*H*), 4.79 (s, 2H, Pyrr*H*), 3.94 (s, 2H, Pyrr*H*), 2.17 (s, 18H, ArCH_3), 2.07 (s, 9H, ArCH_3). UV−vis (benzene) λ_{max}, nm (ε): 433 (1300). Anal. Calcd for $C_{46}H_{48}BFeN_7{\cdot}H_2O$: C, 70.51; H, 6.43; N, 12.51. Found: C, 70.58; H, 6.35; N, 12.41.

Kinetic Measurements. Kinetic measurements were carried out using UV−vis spectroscopy. All kinetic runs were made under pseudo-first-order conditions. A 0.5 mM solution of **1** (5×10^{-4} μmol) in 1 mL of benzene was placed in a 3 cm UV−vis cuvette at 20 °C, followed by injection of 100 equiv of 1,3-cyclohexadiene or 1,4-cyclohexadiene. The progress of the reactions was monitored by following the decrease in absorbance of **1** at 445 nm. All measurements were done in triplicate.

Detection of Organic Products. Reaction progress was monitored by ^{1}H NMR spectroscopy at 70 °C, and the organic products were determined by GC-MS. A 20 mg (28 μmol) amount of **1** in 0.6 mL of C_6D_6 was added to a J. Young NMR tube. After injecting 1 equiv of 1,3-cyclohexadiene or 1,4-cyclohexadiene, reactions were monitored by ^{1}H NMR spectroscopy. When **1** was completely consumed, the reaction mixture was passed through a short aluminum oxide column and eluted with THF. An aliquot of the solution was analyzed by GC-MS to identify the organic products.

X-ray Crystallography. An orange rod-like specimen of $C_{50}H_{58}BFeN_7O$, approximate dimensions 0.143 mm × 0.330 mm × 0.460 mm, was used for X-ray crystallographic analysis. X-ray intensity data were measured on a Bruker Kappa APEX II CCD system equipped with a graphite monochromator and a Mo Kα fine-focus tube (λ = 0.71073 Å).

The total exposure time was 10.00 h. Frames were integrated with the Bruker SAINT software package using a narrow-frame algorithm. Integration of the data using a triclinic unit cell yielded a total of 21 981 reflections to a maximum θ angle of 25.47° (0.83 Å resolution), of which 9471 were independent (average redundancy 2.321, completeness = 98.7%, R_{sig} = 11.24%) and 5414 (57.16%) were greater than $2\sigma(F^2)$. Final cell constants of a = 12.0382(17) Å, b = 12.4997(17) Å, c = 17.915(3) Å, α = 83.989(10)°, β = 74.650(10)°, γ = 85.987(9)°, and volume = 2582.8(7) Å^3 are based upon refinement of the *XYZ* centroids of 4694 reflections above 20 $\sigma(I)$ with 4.717° < 2θ < 49.99°. Data were corrected for absorption effects using the multiscan method (SADABS). The ratio of minimum to maximum apparent transmission was 0.830. The calculated minimum and maximum transmission coefficients (based on crystal size) are 0.8630 and 0.9540.

The structure was solved and refined using the Bruker SHELXTL Software Package using the space group *P*-1, with Z = 2 for the formula unit, $C_{50}H_{58}BFeN_7O$. Non-hydrogen atoms were refined anisotropically. Hydrogen atoms were placed in geometrically calculated positions with U_{iso} = 1.2U_{equiv} of the parent atom (U_{iso} = 1.5U_{equiv} for methyl groups). In addition to one well-behaved solvent molecule, there was also some disordered solvent that was accounted for using SQUEEZE (49 e$^-$ per 461 Å^3 void). Final anisotropic full-matrix least-squares refinement on F^2 with 552 variables converged at R1 = 6.34% for the observed data and wR2 = 17.28% for all data. The goodness-of-fit was 0.975. The largest peak in the final difference electron density synthesis was 0.380 e$^-$/Å^3, and the largest hole was −0.354 e$^-$/Å^3 with an RMS deviation of 0.065 e$^-$/Å^3. On the basis of the final model, the calculated density was 1.080 g/cm^3 and F(000), 892 e$^-$.

Density Functional Theory Calculations. Density functional theory (DFT) calculations were performed using the quantum chemical program Gaussian 09 (G09).[14] Most calculations were carried out employing the B3LYP hybrid functional and the standard

dx.doi.org/10.1021/ic5010006 | Inorg. Chem. 2014, 53, 8425−8430

6-31+G* basis set. Electronic energies and molecular frequencies were computed for the fully optimized structures in the gas phase. Gibbs free energies for different compounds in the gas phase were computed by including the entropic contribution, which contains vibration (within a harmonic approximation, using the calculated vibrational frequencies), rotation (within a rigid rotor approximation), and translation. This is part of the standard output of Gaussian 09 after a frequency analysis. In the cases where the spin states of the iron complexes are not known, geometry optimizations and free energy calculations were performed for several of the most possible spin states. For each species the spin state with the lowest gas-phase free energy was chosen. Data for all spin states of all species are provided in the Supporting Information. Unrestricted DFT was used to investigate the iron complexes with nonzero spin. Spin contaminations were estimated from deviations of the computed $\langle S^2 \rangle = S(S + 1)$ with respect to the corresponding theoretical values and found to be small for all cases in our study.

The total free energies of different intermediates in the THF solution were calculated using the polarizable continuum model (PCM) implemented in Gaussian 09. Bond atomic radii were used to model explicit hydrogen atoms. PCM calculations were carried out for optimized geometries in the gas phase. Geometry optimizations were also performed in the PCM solution. The differences in energies were found to be negligible compared with those performed with the gas-phase-optimized structures. Solvation free energy for a particular complex was computed by subtracting the gas-phase DFT energy from the corresponding PCM energy. This term is then added to the free energy for the gas-phase calculation to obtain the total free energy of this species in the corresponding solution

$$\Delta G_{solution} = \Delta G_{gas\ phase} + \Delta G_{solvation}$$

Due to the prohibitive computational cost of frequency calculations using the 6-31+G* basis set, the gas-phase free energy for each compound was obtained via a frequency calculation for the optimized structure using the 6-31G* basis set. It is expected that addition of the diffuse functions will mostly change the electronic energies of the anions but have a minimal effect on the gas-phase free energies and/or energies for neutral species. This is confirmed through our test calculations.

RESULTS AND DISCUSSION

The iron(IV) nitrido complex **1** reacts cleanly with stoichiometric 1,3-cyclohexadiene at 70 °C to afford the pyrrolide complex PhB(MesIm)$_3$Fe(η^5-C$_4$H$_4$N) **2** in high yield (Scheme 2). Complex **2** has been characterized by

Scheme 2

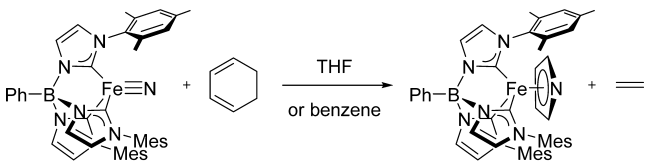

1 **2**

single-crystal X-ray diffraction (Figure 1). The molecular structure reveals a coordinatively saturated metal center that is bound to a κ^3-tris(carbene)borate and an η^5-pyrrolide ligand. The Fe–C/N (pyrrolide) bond lengths (Fe–N 2.106(4) Å; Fe–C 2.100(4)–2.130(4) Å) are longer than other structurally characterized iron(II) pyrrolide complexes (Fe–C 2.000–2.089 Å, Fe–N 2.017–2.087 Å)[15] likely due to the steric pressure imparted by the mesityl groups of the tris(carbene)borate ligand. The pyrrolide ligand is essentially parallel with the plane created by the three carbon atoms of the tris(carbene)borate ligand (angle between planes = 1.8(1)°). The Fe–C (tris-

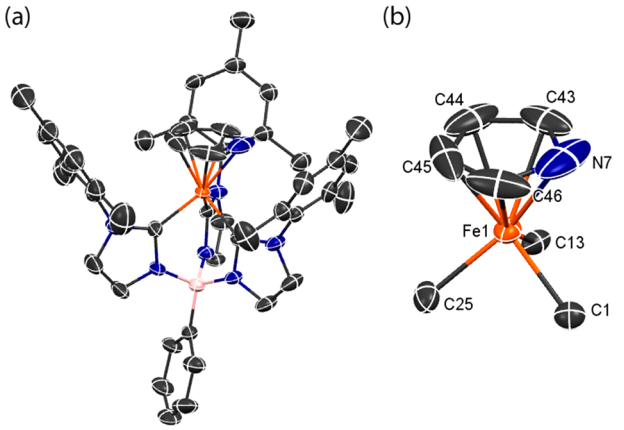

Figure 1. ORTEP diagram showing the structure of **2**. Hydrogen atoms were omitted for clarity; thermal ellipsoids are shown at 50% probability. (a) Full molecule. (b) Most of the tris(carbene)borate ligand omitted for clarity. Selected bond lengths (Angstroms) and angles (degrees): Fe(1)–C(1) 1.957(3); Fe(1)–C(13) 1.970(3); Fe(1)–C(25) 1.942(4); Fe(1)–N(7) 2.106(4); Fe(1)–C(43) 2.130(4); Fe(1)–C(44) 2.117(4); Fe(1)–C(45) 2.100(4); Fe(1)–C(46) 2.114(4); C(1)–Fe(1)–C(13) 86.4(1); C(1)–Fe(1)–C(25) 88.7(2); C(13)–Fe(1)–C(25) 87.3(2).

(carbene)borate) bond lengths (1.937(4)–1.969(3) Å) are similar to other low-spin Fe(II) complexes of this ligand.[11,12]

The complex has been characterized in solution by ^{1}H NMR spectroscopy. Spectral data are consistent with the structure observed in the solid state. All resonances are observed between 0 and 10 ppm, consistent with the low-spin Fe(II) formulation suggested by the metrical data. Two resonances are observed for the protons of the pyrrolide ligand (δ 4.79, 3.94 ppm), consistent with rapid rotation of this ligand on the ^{1}H NMR time scale.

Formation of ethylene (δ = 5.25 ppm) is observed when reaction of **1** and 1,3-cyclohexadiene is monitored by ^{1}H NMR spectroscopy. Conversion of **1** to **2** is found to be quantitative with no observation of reaction intermediates. An isosbestic point is observed at 418 nm when the reaction between **1** and 1,3-cyclohexadiene is monitored by UV–vis spectroscopy under pseudo-first-order conditions.[16] Pseudo-first-order rate constants are proportional to [1,3-CHD], corresponding to the rate law, rate = k_2[**1**][1,3-CHD] (k_2 = 2.2(1) × 10^{-5} M^{-1} s^{-1}).

Building on previous mechanistic proposals,[7] we propose that formation of **2** occurs by the mechanism shown in Scheme 3. A rate-determining [4 + 1] reaction between complex **1** and 1,3-cyclohexadiene provides azabicyclic intermediate **3**, analogously to the reaction of TpOs(N)Cl$_2$ with 1,3-cyclohexadienes.[7] In contrast to this earlier work, where the azabicyclic complex is the final product, we propose a second step in which **3** undergoes a retro Diels–Alder reaction to yield the pyrrolide complex **2** along with an equivalent of ethylene. This step likely does not occur in the reaction of TpOs(N)Cl$_2$ since the azabicylic complex is already coordinatively and electronically saturated.

Surprisingly, similar reaction of **1** with 1,4-cyclohexadiene also produces **2**, although in substantially lower yield (ca. 30%). While no other iron-containing products could be identified, ^{1}H NMR spectroscopy and GC/MS reveal formation of benzene, 1,3-cyclohexadiene, and ethylene (Scheme 4). Importantly, there is no 1,3-cyclohexadiene impurity in the 1,4-cyclohexadiene substrate. In addition, formation of a

dx.doi.org/10.1021/ic5010006 | Inorg. Chem. 2014, 53, 8425–8430

Scheme 3. Proposed Mechanism of Reaction between 1 and 1,3-Cyclohexadiene

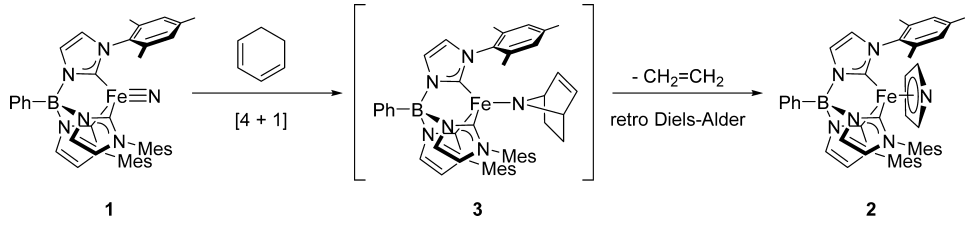

Scheme 4

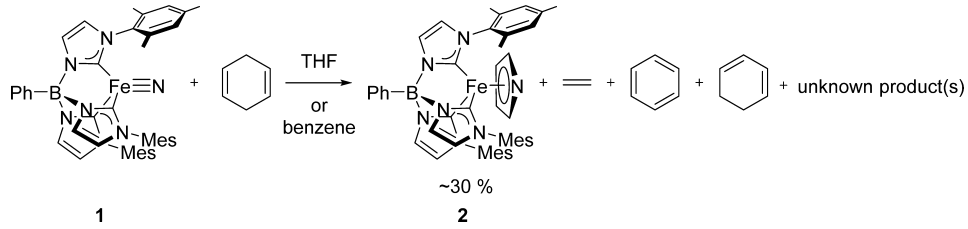

number of unidentified species is observed when the reaction is monitored by ^{1}H NMR spectroscopy. The kinetics, as monitored by UV–vis spectroscopy (20 °C, [Fe] = 0.5 mM and [1,4-CHD] = 500 mM), are not as well behaved as for 1,3-cyclohexadiene, and no isosbestic points are observed in the kinetic traces.[16] While the kinetic data was not of sufficient quality to allow for reliable determination of rate constants, reaction with 1,4-cyclohexadiene is qualitatively slower than with 1,3-cyclohexadiene. Additionally, the reaction with deuterated 1,4-cyclohexadiene is qualitatively slower than with the nondeuterated substrate.

Formation of benzene suggests that the reaction involves hydrogen-atom abstraction from 1,4-cyclohexadiene; however, formation of 1,3-cyclohexadiene is not so obvious. Low-valent complexes and very basic late metal amido complexes have been reported to catalyze cyclohexadiene isomerization through mechanisms involving metal hydrides[17] and proton transfer,[18] respectively; however, it is not clear that similar mechanisms are relevant in the case of **1**. We are unaware of similar isomerization reactions for other metal–ligand multiple bonds.

To obtain insight into the mechanism, we used electronic structure theory, in the form of density function theory (DFT), to calculate the thermodynamics of possible reactions between these **1** and 1,4-cyclohexadiene. Specifically, a square scheme for proton, electron, and hydrogen-atom transfer from 1,4-cyclohexadiene to **1** in THF solvent (Figure 3) reveals that neither proton nor electron transfer to **1** from 1,4-cyclohexadiene is thermodynamically favorable (ΔG > 38 kcal/mol for both pathways). On the other hand, hydrogen-atom transfer to provide the iron(III) imido PhB(MesIm)$_3$Fe≡NH, **4**, and the cyclohexadienyl radical is slightly uphill thermodynamically. Therefore, we suggest that the first step of the reaction involves hydrogen-atom transfer from 1,4-cyclohexadiene to **1**, providing the cyclohexadienyl radical. Hydrogen-atom transfer back to the cyclohexadienyl radical from **4** will regenerate **1** and produce either 1,4-cyclohexadiene or its isomer, 1,3-cyclohexadiene. To evaluate the likelihood of the latter event, we also calculated the thermodynamics for hydrogen-atom transfer from **4** to yield 1,3-cyclohexadiene, finding the reaction to be energetically favorable (ΔG = −3.2 kcal/mol in THF).

We also computationally evaluated the possibility of C–N bond formation between **4** and the cyclohexadienyl radical, yielding the iron(II) rebound product PhB(MesIm)$_3$Fe–N(H)(C$_6$H$_7$) (S = 2). Similar rebound reactions have been observed for pyridine-activated [(salchda)Ru≡N]$^+$.[19] These calculations reveal that formation of the rebound product is thermodynamically favorable (ΔG = −22.4 kcal/mol in THF). Furthermore, abstraction of an additional hydrogen atom to provide the iron(II) amido complex PhB(MesIm)$_3$Fe–NH$_2$ and benzene is also calculated to be thermodynamically favorable ((ΔG = −66.0 kcal/mol in THF). We note that attempts to independently prepare PhB(MesIm)$_3$Fe–NH$_2$ have been unsuccessful.

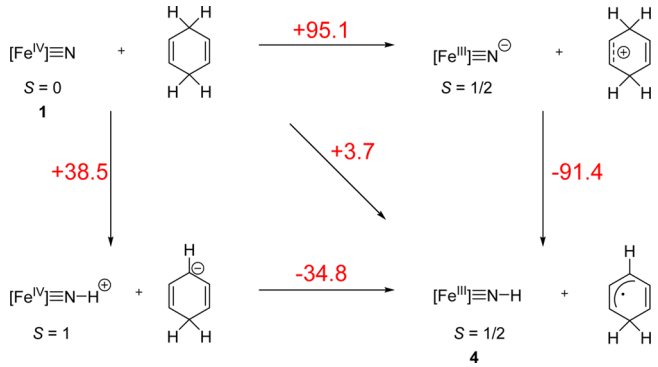

Figure 3. Square scheme for formation of PhB(MesIm)$_3$Fe≡NH **4** by reaction of **1** with 1,4-cyclohexadiene in THF solvent. Lowest energy spin state is shown. Free energy differences are shown in kcal/mol.

In light of the much greater driving force for either formation of the rebound product or additional hydrogen-atom transfer, it is surprising that formation of **2** is observed. It is likely that there are kinetic barriers to these other reactions that have their origin in the electronic structure of the imido complex **4**. In support of this hypothesis, analysis of the frontier orbitals reveals that the SOMO is predominantly iron centered, with little contribution from the imido nitrogen.[16] In addition, almost all of the spin density (84%) is located on iron, with only 6% on the imido nitrogen. Thus, despite the favorable thermodynamics, the electronic structure of the imido intermediate **4** slows both the rebound and the hydrogen-atom transfer reactions.

The experimental and theoretical results lead us to propose a mechanism for reaction of **1** with 1,4-cyclohexadiene (Scheme 5). The first step of the reaction involves hydrogen-atom

dx.doi.org/10.1021/ic5010006 | Inorg. Chem. 2014, 53, 8425–8430

Scheme 5. Proposed Mechanism of Reaction between 1 and 1,4-Cyclohexadiene

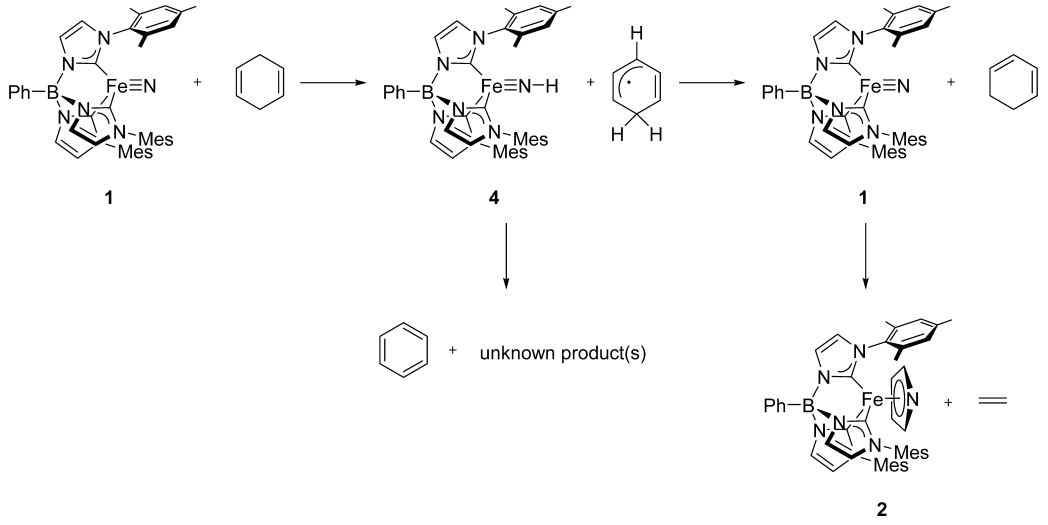

transfer from 1,4-cyclohexadiene to **1**, yielding the iron(III) imido complex **4** and the cyclohexadienyl radical. Hydrogen-atom transfer back to the radical generates 1,3-cyclohexadiene, leading to formation of **2** and ethylene, as described above. In the absence of other iron-mediated pathways, benzene is formed by self-reaction of the cyclohexadienyl radical.[20] It is likely that the imido complex **4** decomposes to a number of species that account for the remaining 70% of iron. While this scheme does not fully describe the entire reaction landscape, it does provide a plausible explanation for formation of the identifiable products of this reaction, in particular, the unanticipated formation of **2**.

In summary, we find that reactions of the nitrido complex **1** with both 1,3- and 1,4-cyclohexadiene provide the pyrrolide complex **2**, albeit in very different yields. In the case of 1,3-cyclohexadiene, we propose the reaction mechanism involves a sequence of two concerted reactions: a [4 + 1] cycloaddition followed by a retro Diels–Alder reaction. In the case of 1,4-cyclohexadiene, we propose that isomerization of the substrate through a cyclohexadienyl radical intermediate yields 1,3-cyclohexadiene, which then reacts with additional **1** to provide **2**. To the best of our knowledge, this radical mechanism is a new pathway for 1,4-cyclohexadiene isomerization.

■ ASSOCIATED CONTENT

Ⓢ Supporting Information

Kinetic traces, computational results, and X-crystallographic data. This material is available free of charge via the Internet at http://pubs.acs.org.

■ AUTHOR INFORMATION

Corresponding Authors

*E-mail: haobin@nmsu.edu.

*E-mail: smith962@indiana.edu.

Present Address

[§]University of Connecticut, Department of Chemistry, Storrs, Connecticut 06269, United States.

Author Contributions

All authors have given approval to the final version of the manuscript.

Notes

The authors declare no competing financial interest.

■ ACKNOWLEDGMENTS

Funding from Indiana University, the Department of Energy–Basic Energy Sciences (DE-FG02-08ER15996), and the Camille and Henry Dreyfus Foundation is gratefully acknowledged. The Bruker X8 X-ray diffractometer was purchased via an NSF CRIF:MU award to The University of New Mexico, CHE-0443580. S.B.M. thanks NSF-AMP (HRD 0929343) and NIH-RISE (R25 GM061222-11) for financial support. H.W. acknowledges support from the NSF (CHE-1012479). This work used resources of the National Energy Research Scientific Computing Center, which is supported by the Office of Science of the U.S. Department of Energy under Contract No. DE-AC02-05CH11231. We thank the reviewers and Prof. J. M. Mayer for insightful comments and suggestions.

■ REFERENCES

(1) Selected reviews and book chapters: (a) Suh, Y.; Seo, M. S.; Kim, K. M.; Kim, Y. S.; Jang, H. G.; Tosha, T.; Kitagawa, T.; Kim, J.; Nam, W. *J. Inorg. Biochem.* **2006**, *100*, 627. (b) Nam, W. *Acc. Chem. Res.* **2007**, *40*, 522. (c) Oldenburg, P. D.; Mas-Ballesté, R.; Que, Jr., L. In *Mechanisms in Homogeneous and Heterogeneous Epoxidation Catalysts*; Oyama, S. T., Ed.; Elsevier: Amsterdam, Netherlands, 2008. (d) Schröder, K.; Junge, K.; Bitterlich, B.; Beller, M. *Top. Organomet. Chem.* **2011**, *33*, 83.

(2) Che, C.-M.; Zhou, C.-Y.; Wong, E. L.-M. *Top. Organomet. Chem.* **2011**, *33*, 111.

(3) Formation of tosyl aziridines via putative imido intermediates: (a) Mansuy, D.; Mahy, J.-P.; Dureault, A.; Bedi, G.; Battioni, P. *J. Chem. Soc., Chem. Commun.* **1984**, 1161. (b) Mahy, J.-P.; Bedi, G.; Battioni, P.; Mansuy, D. *J. Chem. Soc., Perkin Trans. 2* **1988**, 1517. (c) Vyas, R.; Gao, G.-Y.; Harden, J. D.; Zhang, X. P. *Org. Lett.* **2004**, *6*, 1907. (d) Yan, S.-Y.; Wang, Y.; Shu, Y.-J.; Liu, H.-H.; Zhou, X.-G. *J. Mol. Catal. A* **2006**, *248*, 148. (e) Klotz, K. L.; Slominski, L. M.; Hull, A. V.; Gottsacker, V. M.; Mas-Ballesté, R.; Que, L., Jr.; Halfen, J. A. *Chem. Commun.* **2007**, 2063. (f) Nakanishi, M.; Salit, A.-F.; Bolm, C. *Adv. Synth. Catal.* **2008**, *350*, 1835. (g) Klotz, K. L.; Slominski, L. M.; Riemer, M. E.; Phillips, J. A.; Halfen, J. A. *Inorg. Chem.* **2009**, *48*, 801. (h) Liang, S.; Jensen, M. P. *Organometallics* **2012**, *31*, 8055.

(4) Formation of alkyl/aryl aziridines: (a) King, E. R.; Hennessy, E. T.; Betley, T. A. *J. Am. Chem. Soc.* **2011**, *133*, 4917. (b) Cramer, S. A.; Jenkins, D. M. *J. Am. Chem. Soc.* **2011**, *133*, 19342. (c) Hennessy, E. T.; Liu, R. Y.; Iovan, D. A.; Duncan, R. A.; Betley, T. A. *Chem. Sci.* **2014**, *5*, 1526.

(5) Man, W.-L.; Lam, W. W. Y.; Yiu, S.-M.; Lau, T.-C.; Peng, S.-M. *J. Am. Chem. Soc.* **2004**, *126*, 15336.

(6) (a) Brown, S. N. *J. Am. Chem. Soc.* **1999**, *121*, 9752. (b) Maestri, A. G.; Taylor, S. D.; Schuck, S. M.; Brown, S. N. *Organometallics* **2004**, *23*, 1932.
(7) Maestri, A. G.; Cherry, K. S.; Toboni, J. J.; Brown, S. N. *J. Am. Chem. Soc.* **2001**, *123*, 7459.
(8) Smith, J. M.; Subedi, D. *Dalton Trans.* **2012**, *41*, 1423.
(9) (a) Wagner, W.-D.; Nakamoto, K. *J. Am. Chem. Soc.* **1988**, *110*, 4044. (b) Wagner, W.-D.; Nakamoto, K. *J. Am. Chem. Soc.* **1989**, *111*, 1590. (c) Meyer, K.; Bill, E.; Mienert, B.; Weyhermüller, T.; Wieghardt, K. *J. Am. Chem. Soc.* **1999**, *121*, 4859. (d) Grapperhaus, C. A.; Mienert, B.; Bill, E.; Weyhermüller, T.; Wieghardt, K. *Inorg. Chem.* **2000**, *39*, 5306. (e) Aliaga-Alcalde, N.; DeBeer George, S.; Mienert, B.; Bill, E.; Wieghardt, K.; Neese, F. *Angew. Chem., Int. Ed.* **2005**, *44*, 2908. (f) Petrenko, T.; DeBeer George, S.; Aliaga-Alcalde, N.; Bill, E.; Mienert, B.; Xiao, Y.; Guo, Y.; Sturhahn, W.; Cramer, S. P.; Wieghard, K.; Neese, F. *J. Am. Chem. Soc.* **2007**, *129*, 11053. (g) Berry, J. F.; Bill, E.; Bothe, E.; DeBeer George, S.; Mienert, B.; Neese, F.; Wieghardt, K. *Science* **2006**, *312*, 1937. (h) Schlangen, M.; Neugebauer, J.; Reiher, M.; Schröder, D.; Pitarch Lopez, J.; Haryono, M.; Heinemann, F. W.; Grohmann, A.; Schwarz, H. *J. Am. Chem. Soc.* **2008**, *130*, 4285. (i) Boyd, J. P.; Schlangen, M.; Grohmann, A.; Schwarz, H. *Helv. Chim. Acta* **2008**, *91*, 1430. (j) Torres-Alacan, J.; Das, U.; Filippou, A. C.; Vöhringer, P. *Angew. Chem., Int. Ed.* **2013**, *49*, 12833.
(10) Scepaniak, J. J.; Young, J. A.; Bontchev, R. P.; Smith, J. M. *Angew. Chem., Int. Ed.* **2009**, *48*, 3158.
(11) (a) Scepaniak, J. J.; Harris, T. D.; Vogel, C. S.; Sutter, J.; Meyer, K.; Smith, J. M. *J. Am. Chem. Soc.* **2011**, *133*, 3824. (b) Scepaniak, J. J.; Margarit, C. G.; Harvey, J. N.; Smith, J. M. *Inorg. Chem.* **2011**, *50*, 9508.
(12) Scepaniak, J. J.; Bontchev, R. P.; Johnson, D. L.; Smith, J. M. *Angew. Chem., Int. Ed.* **2011**, *50*, 6630.
(13) Goldsmith, C. R.; Jonas, R. T.; Stack, T. D. P. *J. Am. Chem. Soc.* **2002**, *124*, 83.
(14) Frisch, M. J.; Trucks, G. W.; Schlegel, H. B.; Scuseria, G. E.; Robb, M. A.; Cheeseman, J. R.; Scalmani, G.; Barone, V.; Mennucci, B.; Petersson, G. A.; Nakatsuji, H.; Caricato, M.; Li, X.; Hratchian, H. P.; Izmaylov, A. F.; Bloino, J.; Zheng, G.; Sonnenberg, J. L.; Hada, M.; Ehara, M.; Toyota, K.; Fukuda, R.; Hasegawa, J.; Ishida, M.; Nakajima, T.; Honda, Y.; Kitao, O.; Nakai, H.; Vreven, T.; Montgomery, Jr., J. A.; Peralta, J. E.; Ogliaro, F.; Bearpark, M.; Heyd, J. J.; Brothers, E.; Kudin, K. N.; Staroverov, V. N.; Kobayashi, R.; Normand, J.; Raghavachari, K.; Rendell, A.; Burant, J. C.; Iyengar, S. S.; Tomasi, J.; Cossi, M.; Rega, N.; Millam, N. J.; Klene, M.; Knox, J. E.; Cross, J. B.; Bakken, V.; Adamo, C.; Jaramillo, J.; Gomperts, R.; Stratmann, R. E.; Yazyev, O.; Austin, A. J.; Cammi, R.; Pomelli, C.; Ochterski, J. W.; Martin, R. L.; Morokuma, K.; Zakrzewski, V. G.; Voth, G. A.; Salvador, P.; Dannenberg, J. J.; Dapprich, S.; Daniels, A. D.; Farkas, Ö.; Foresman, J. B.; Ortiz, J. V.; Cioslowski, J.; Fox, D. J. *Gaussian 09*, Revision A.1; Gaussian, Inc.: Wallingford, CT, 2009.
(15) (a) Pyshnograeva, N. I.; Setkina, V. N.; Batsanov, A. S.; Struchkov, Yu.T. *J. Organomet. Chem.* **1985**, *288*, 189. (b) Kuhn, N.; Jendral, K.; Boese, R.; Blaser. *Chem. Ber.* **1991**, *124*, 89. (c) Hansen, J. G.; Søtofte, I.; Johannsen, M. *Org. Lett.* **2001**, *3*, 499. (d) Lo, M.M.-C.; Fu, G. C. *J. Am. Chem. Soc.* **2002**, *124*, 4572. (e) Kowalski, K.; Jakrzewski, J.; Jerzykiewicz, L. *J. Organomet. Chem.* **2005**, *690*, 764. (f) Kowalski, K.; Winter, R. F. *J. Organomet. Chem.* **2008**, *693*, 2181. (g) Fukuda, T.; Koga, Y.; Iwao, M. *Heterocycles* **2008**, *76*, 1237. (g) Kowalski, K.; Winter, R. F. *J. Organomet. Chem.* **2009**, *694*, 1041. (h) Brunker, T. J.; Roembke, B. T.; Golen, J. A.; Rheingold, A. L. *Organometallics* **2011**, *30*, 2272.
(16) See Supporting Information for details.
(17) (a) Karel, K. J.; Brookhart, M.; Aumann, R. *J. Am. Chem. Soc.* **1981**, *103*, 2695. (b) Esteruelas, M. A.; Sola, E.; Oro, L. A.; Werner, H.; Meyer, U. *J. Mol. Catal.* **1989**, *53*, 43. (c) Qian, Y.; Guisheng, L.; Zheng, X.; Huang, Y.-Z. *J. Mol. Catal.* **1993**, *78*, L31. (d) Ohff, A.; Burlakov, V. V.; Rosenthal, U. *J. Mol. Catal. A* **1996**, *105*, 103. (f) Mathers, R. T.; Shreve, M. J.; Meyler, E.; Damodaran, K.; Iwig, D. F.; Kelley, D. J. *Macromol. Rapid Commun.* **2011**, *32*, 1338. (f) Mao, J. X.; Mathers, R. T.; Damodaran, K. *J. Organomet. Chem.* **2013**, *741*–*742*, 15.
(18) (a) Holland, A. W.; Bergman, R. G. *J. Am. Chem. Soc.* **2002**, *124*, 14684. (b) Conner, D.; Jayaprakash, K. N.; Wells, M. B.; Manzer, S.; Gunnoe, T. B.; Boyle, P. D. *Inorg. Chem.* **2003**, *42*, 4759. (c) Fox, D. J.; Bergman, R. G. *Organometallics* **2004**, *23*, 1656.
(19) Man, W.-L.; Lam, W. W. Y.; Kwong, H.-K.; Yiu, S.-M.; Lau, T.-C. *Angew. Chem., Int. Ed.* **2012**, *51*, 9101.
(20) (a) Sauer, M. C., Jr.; Ward, B. *J. Phys. Chem.* **1967**, *71*, 3971. (b) James, D. G. L.; Suart, R. D. *Trans. Faraday Soc.* **1968**, *64*, 2752. (c) Berho, F.; Rayez, M.-T.; Lesclaux, R. *J. Phys. Chem. A* **1999**, *103*, 5501.